A Multiresponsive Calix[6]arene Pseudorotaxane Empowered by Fluorophoric Dansyl Groups

Leonardo Andreoni,[a, b] Giovanni Mariano Beneventi,[a] Gabriele Giovanardi,[c] Gianpiero Cera,*[c] Alberto Credi,[b, d] Arturo Arduini,[c] Andrea Secchi,*[c] and Serena Silvi*[a, b]

Abstract: We report the synthesis and characterization, by means of NMR and UV-visible spectroscopy and electrochemical techniques, of a dansyl calix[6]arene derivative and of its pseudorotaxane complex with a bipyridinium-based axle. This novel macrocycle shows remarkable complexation ability, in analogy with parent compounds, while the dansyl moieties impart valuable features to the system. Indeed, these units: i) signal the state of the system by fluorescence; ii) can be reversibly protonated, enabling the modulation of the complexation abilities of the macrocycle; iii) participate in photoinduced electron transfer processes, which may be exploited to tune the stability of the supramolecular complex. Therefore, in this multiresponsive pseudorotaxane, the threading and de-threading motions of the molecular components can be modulated either by protonation of the calixarene host or by reduction of the bipyridinium guest, which can be accomplished both by electrochemical reduction and via photoinduced electron transfer. Overall, three orthogonal and reversible stimuli can be used to induce molecular movements of the pseudorotaxane components.

Introduction

The ability of a system to respond to multiple stimuli, i.e., multiresponsiveness, can result from a single unit being able to switch according to different stimuli,[1] as well as from the combination of molecular switches.[2] The synthesis of multiresponsive molecular components able to perform several programmed functions can give impetus to the implementation of novel artificial nano-machines and devices.[3] In this context, the synthetic versatility of heteroditopic calix[6]arene wheels has already been exploited to construct several interlocked and interwoven supramolecular structures.[4] The proper choice of the hydrogen-bonding donor moiety on the upper rim of the calix[6]arene scaffold enables to control both the complexation features and the threading process of this class of compounds.[5] With the aim to expand the working mode of these compounds and incorporate new functions, we recently introduced a new class of heteroditopic wheels functionalised with three sulphonamide moieties,[6] prompted by the abundance and the synthetic modularity of the sulphonyl group.[7] A strong association with bipyridinium-based axles was observed and, based on these results, we designed a new dansyl-functionalised[8] sulphonated heteroditopic calix[6]arene **TDA** (Scheme 1).

The dansyl group is a widely employed fluorophore whose easy derivatisation, particularly with the calixarene scaffold, fostered its use for the synthesis of fluorescent chemosensors.[9]

[a] L. Andreoni, G. M. Beneventi, Prof. S. Silvi
Dipartimento di Chimica "G. Ciamician"
Università di Bologna
Via Selmi 2, 40126, Bologna (Italy)
E-mail: serena.silvi@unibo.it
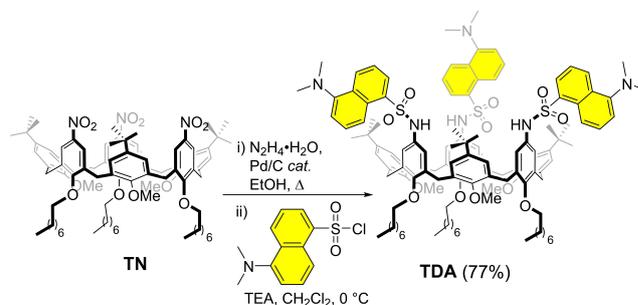Homepage: https://www.unibo.it/sitoweb/serena.silvi/en

[b] L. Andreoni, Prof. A. Credi, Prof. S. Silvi
CLAN-Center for Light Activated Nanostructures
Istituto per la Sintesi Organica e la Fotoreattività
Consiglio Nazionale delle Ricerche
Via Gobetti 101, 40129 Bologna (Italy)

[c] G. Giovanardi, Prof. G. Cera, Prof. A. Arduini, Prof. A. Secchi
Dipartimento di Scienze Chimiche della Vita e della Sostenibilità Ambientale
Università di Parma
Parco Area delle Scienze 17/A, 43124 Parma (Italy)
E-mail: gianpiero.cera@unipr.it
        andrea.secchi@unipr.it
Homepage: https://personale.unipr.it/en/ugovdocenti/person/203179
          https://personale.unipr.it/en/ugovdocenti/person/19180

[d] Prof. A. Credi
Dipartimento di Chimica Industriale "Toso Montanari"
Università di Bologna
Viale del Risorgimento 4, 40136 Bologna (Italy)

Scheme 1. Synthesis of tridansylamido calix[6]arene **TDA**.

Chem. Eur. J. **2023**, 29, e202203472 (1 of 7)

© 2023 The Authors. Chemistry - A European Journal published by Wiley-VCH GmbH

When anchored to a supramolecular host, it provides several attractive features such as (i) a strong fluorescence, (ii) a relatively long emission wavelength with a large Stokes shift, (iii) sensitivity to the polarity of the medium.[10] The fluorescence of the dansyl moiety represents an additional tool for assessing the supramolecular host-guest interactions.[11] Furthermore, the amine units of the dansyl group can undergo protonation reactions,[12] which can be exploited to alter the complexation properties of the macrocycle. As it is well known that pseudorotaxanes based on the calixarene-bipyridinium recognition motif can be destabilised by reduction of the guest component, the disassembly of the supramolecular complex could be obtained both by electrochemical reduction[5] and

photoinduced electron transfer from the dansyl units.[13] Overall, our aim is to exploit the versatility of the newly devised wheel in a multiresponsive pseudorotaxane system[2] operated by three different, orthogonal, and reversible stimuli, acting on both the ring and the axle (Figure 1).
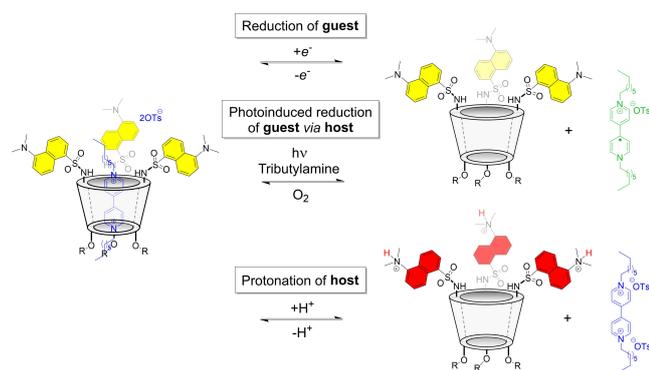
Results and Discussion

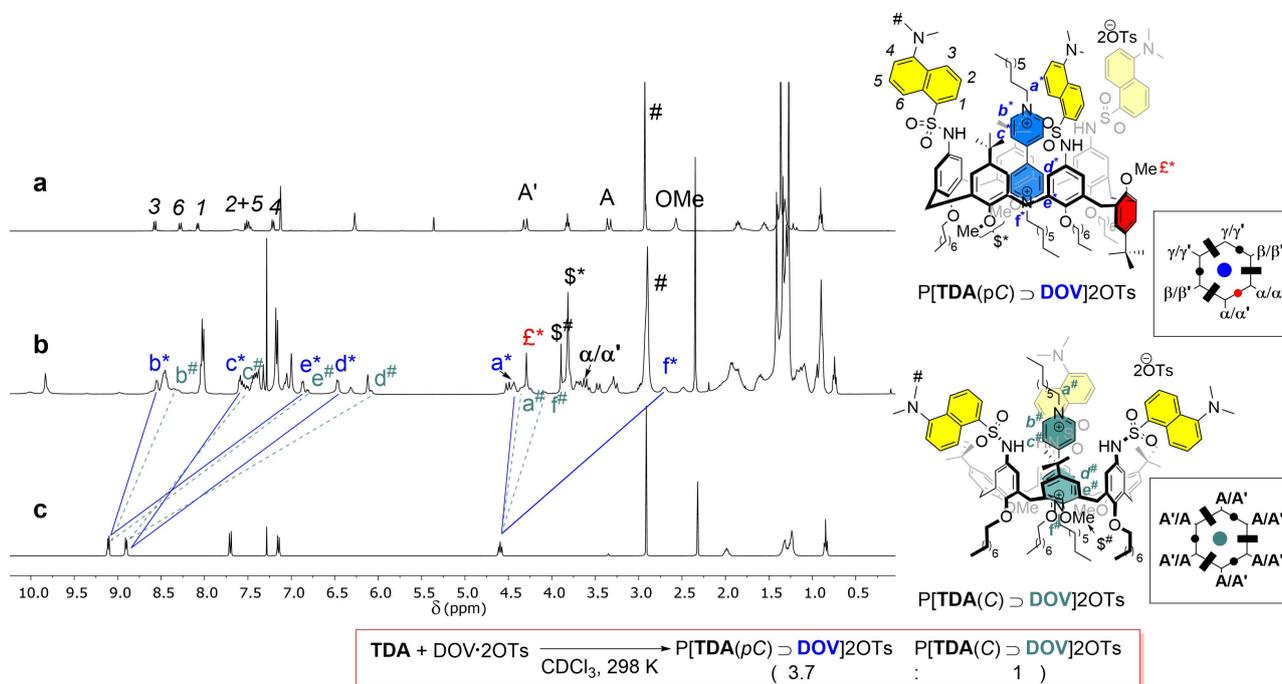### Synthesis and characterisation of pseudorotaxanes

The synthesis of the tridansylamido calix[6]arene **TDA** was performed following established protocols, starting from the known trioctyloxy trinitro derivative **TN** (Scheme 1).[14]

The conformation adopted by **TDA** was studied by NMR analysis, and it presents strong analogies to the family of its sulphonamido counterparts. Particularly, in low polarity solvents, **TDA** adopts a *pseudo cone* conformation, defining a trigonal prism characterised by several diagnostic signals. An AX system of two doublets A/A' with a geminal coupling of $^2J = 15.4$ Hz of the methylene groups of calix[6]arene ring and an upfield-shifted resonance (2.6 ppm) for the methoxy groups which point inside the aromatic cavity. The high symmetry of the system was finally confirmed by a sharp singlet for the dimethylamino groups (#) at 2.93 ppm (Figure 2a).

The complexation features of **TDA** were evaluated by equilibrating a 5 mM solution of the calixarene with the tosylate salt of 1,1'-dioctyl-4,4'-bipyridinium (**DOV**·2OTs) at 298 K (1:1 in CDCl$_3$). Analysis by ^{1}H NMR revealed the formation of two

Figure 1. Aim of this work: Synthesis of a multiresponsive calix[6]arene-based pseudorotaxane system enabled by dansyl groups.

Figure 2. ^{1}H NMR spectra (400 MHz, 298 K) of a) **TDA** in CD$_2$Cl$_2$, b) pseudorotaxane P[**TDA**⊃**DOV**]2OTs in CDCl$_3$, (c) **DOV**·2OTs in CD$_3$OD. Right-up, schematic representation of P[**TDA**(p*C*)⊃**DOV**]2OTs, right-down P[**TDA**(p*C*)⊃**DOV**]2OTs. The colour of the ovals/rectangles shows the relative position of the phenolic substituent with respect to the plane defined by the bridging methylene groups (hexagon), i.e., black upward, red downward. The rectangle identifies the phenolic ring substituted with the octyloxy chains, while the circle those with the methoxy groups.

Chemistry–A European Journal

Research Article
doi.org/10.1002/chem.202203472

Chemistry Europe
European Chemical
Societies Publishing

pseudorotaxane species in solution (3.7:1 determined by ^{1}H NMR integration of threaded aromatic CH signals of the bipyridinium guest). The major one was assigned to an interwoven structure in which **TDA** assumes a *partial cone* (*pC*) conformation P[**TDA**(*pC*)⊃**DOV**]2OTs with an inversion point associated with a ring bearing a methoxy group (Figure 2b). This geometry was confirmed by its typical NMR pattern, which includes: i) a down-field shift of the methoxy groups that gave rise to two signals in a 1:2 ratio (£*+$*); ii) the split of the two doublets (ax+eq) A/A' of the methylene bridge in **TDA** into six doublets, with geminal coupling, in a 1:1 ratio; iii) a significant shift of the ^{13}C resonances for the α/α' couple to δ=35.6 ppm (Figure S13 in Supporting Information).[15] Further NMR investigation allowed us to confirm the geometry of the second minor species as the *cone* (*C*) conformer P[**TDA**(*C*)⊃**DOV**]2OTs (Figures S16 and S17).

The effect of the protonation on the complexation features of the pseudorotaxane system was subsequently investigated. The addition of three equivalents of triflic acid (TfOH) to a solution of **TDA** in CDCl₃ (5 mM) resulted in a general broadening of the ^{1}H NMR resonances and, particularly, a slight down-field shift of the dimethylamino signals (#) at 3.00 ppm which confirmed the exhaustive protonation of the system (Figure 3a). Nonetheless, the wheel is still present as a major *pseudo cone* conformer, as confirmed by its typical AX system for the methylene bridging protons A/A'. Subsequently, the resulting solution of **TDA**·3HOTf was equilibrated with **DO-**
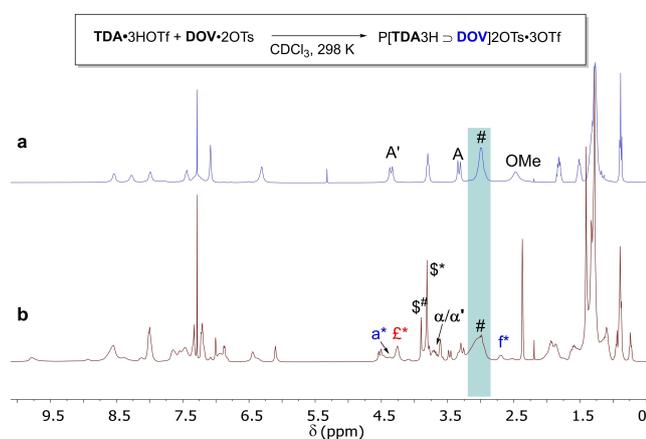
V·2OTs (1 equiv.) and analysed by NMR spectroscopy (Figure 3b). Interestingly, the common features for P[**TDA**3H ⊃**DOV**]2OTs·3OTf, in which the calix[6]arene wheel is present as a mixture of a major *partial cone* and a minor *cone* conformer, were fully retained (Figure 3b and Figures S16 and S17). However, the presence of broader signals, particularly the one related to the dimethylamino groups (#) (Figure 3b), indicates a higher degree of conformational freedom for the interwoven structure and an expected change of the kinetic regime of the complexation from slow to fast exchange on the NMR timescale.[16] In order to gain more insight on the complexation abilities of the protonated wheel, we run variable temperature (VT) NMR experiments (see Figure S18). Nevertheless, we never observed sharp signals both at high and low temperatures. Hence, we decided to get more insights into the features of the newly devised pseudorotaxane system by means of spectroscopical investigations.

Photophysical characterisation: chemically induced de-threading

The photophysical characterisation of **TDA** was performed in CH₂Cl₂, and the data are gathered in Table 1. The absorption and luminescence spectral features of **TDA** reflect the sum of its components, that is, the calixarene scaffold and the three dansyl moieties, as inferred by comparison with the model 5-(dimethylamino)naphthalene-1-sulfonamide (**1**) (Table 1). Indeed, the typical absorption and luminescence bands of dansyl are preserved, at $\lambda_{abs}=343$ nm and $\lambda_{em}=514$ nm, respectively, with a quantum yield of 0.46.

Upon addition of TfOH to **TDA**, the expected spectral changes related to the protonation of the dansyl units[12,17] are observed (Figure 4): both the absorption and luminescence bands shift to higher energies, and the emission quantum yield decreases to 8×10^{-4} (Table 1). Two isosbestic points are maintained throughout the experiment, and the titration curve reaches a plateau after the addition of three equivalents of acid, thus suggesting that the three dansyl units are all protonated and independent from one another. The reaction is fully reversible, as the spectral features of **TDA** are completely restored upon the addition of a base (Figure S27).

Upon titration of **TDA** with **DOV**·2OTs the absorption spectrum shows small changes on the dansyl band (Figure 5a): the expected charge transfer band arising from the interaction between the **DOV** guest and the calixarene cavity,[5,18] is hidden
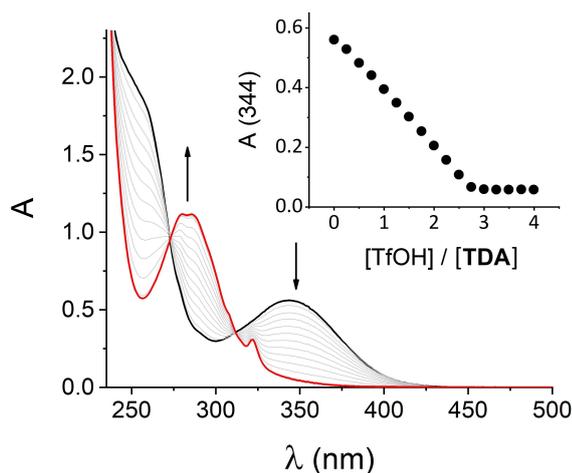

Figure 3. ^{1}H NMR stack plot (400 MHz, CDCl₃) showing the effect of the protonation of the dansyl moieties in a) **TDA** and b) its pseudorotaxane complex with **DOV**·2OTs.

Table 1. Photophysical data of the investigated compounds.

Compound	Absorption		Emission		
	λ_{max}	ε [M⁻¹ cm⁻¹]	λ_{max}	τ [ns]	ϕ_{em}
(structure)	255	14500	508	16.1	0.61
	343	4400			
TDA	256[a]	40200	514	15.2	0.46
	343	12600			
TDA·3HOTf	283	24500	313	\	8×10^{-4}

[a] Shoulder of the absorption band.

Chem. Eur. J. **2023**, *29*, e202203472 (3 of 7)

© 2023 The Authors. Chemistry - A European Journal published by Wiley-VCH GmbH

Figure 4. Absorption spectra of a CH₂Cl₂ solution of **TDA** (4.0×10^{-5} M) upon titration with TfOH. The inset shows the plot of the absorption changes at 344 nm.

Table 2. Thermodynamic and kinetic constants of the investigated compounds.			
Compound	logK$_{eq}$[a]	k$_{thr}$[b] [10^4 M^{-1}s^{-1}]	k$_{dethr}$[c] [s^{-1}]
[**TDA**⊃**DOV**]2OTs	6.9	27	0.034
[**TDA3H**⊃**DOV**]2OTs·3OTf	5.1	8.7	0.69

[a] Equilibrium constant; [b] rate constant of the forward (threading) reaction; [c] rate constant of the backward (de-threading) reaction.

beneath the absorption band of the dansyl moieties, which undergoes a slight red shift. The luminescence is quenched (Figure 5b), most likely because of the photoinduced electron transfer from the dansyl units to the bipyridinium guest.[13,19]
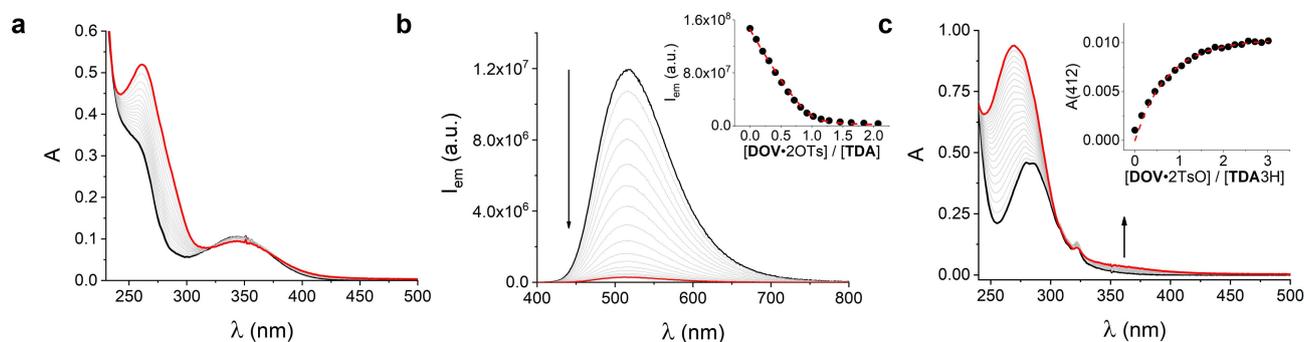
Upon fitting the data with a 1:1 model, an association constant as large as 8×10^6 M^{-1} is obtained (Figure 5b and Table 2), in analogy with parent triphenylureido calix[6]arene.[5] On the other hand, upon titration of the protonated **TDA** with **DOV**·2OTs the appearance of the charge transfer band can be detected just below 400 nm (Figure 5c). Upon fitting these data, an association constant of 1.3×10^5 M^{-1} is obtained (Table 2). This drop in the stability of the supramolecular adduct is not unexpected and it could be ascribed to two effects: i) the presence of the triflate anions, which could partially affect the ion pair equilibria and the coordination ability of the sulphonamide units of **TDA**; ii) the electrostatic repulsion between the doubly charged bipyridinium guest and the triply charged protonated host.

To assess the extent of each contribution, we investigated the role of the triflate anion. Upon the addition of three equivalents of tetrabutylammonium triflate (TBAOTf) to a 1:1 mixture of **TDA** and **DOV**·2OTs, only a small increase in the emission spectra was observed (Figure S34), which is not compatible with a decrease of the association constant of almost two orders of magnitude. Therefore, the large decrease in the stability of the pseudorotaxane is mainly ascribed to the protonation of **TDA**. The protonation of the host-guest complex was also investigated. Indeed, similar spectral changes were observed as on **TDA** alone, thus suggesting that the acid-base properties are maintained in the adduct (Figure S35). Unfortunately, given the small spectral changes associated with the complexation / decomplexation processes and the large variations due to protonation/deprotonation reactions, it is not possible to directly observe the dissociation of the complex upon protonation.

Kinetic experiments were performed by mixing **TDA** or protonated **TDA** with **DOV**·2OTs. In both cases, the absorption vs. time curves were fitted with a mixed order reaction, i.e., a forward second-order and a backward first-order reaction and fixing the value of the equilibrium constant (Table 2). In general, the effect of protonation of **TDA** on kinetics is less pronounced than on thermodynamics, and it is more relevant to the de-threading reaction, which is 20 times faster for the protonated pseudorotaxane.
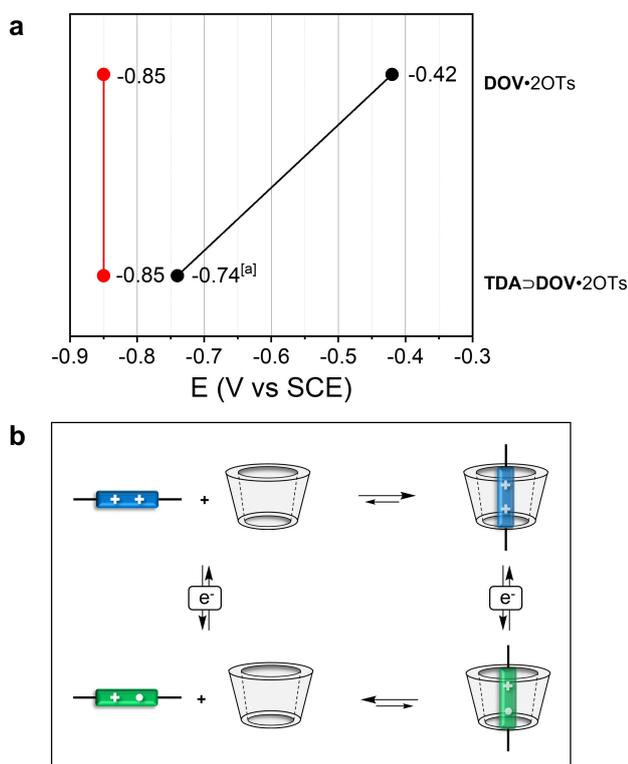

Figure 5. (a-b) Absorption and emission spectra (λ$_{ex}$ = 343 nm) of a CH₂Cl₂ solution of **TDA** (8.2×10^{-6} M) upon titration with **DOV**·2OTs. The inset shows the titration curve (black dots) together with the fitting of the data (dashed line). In Figure 5a, the increase of absorbance at 260 nm is due to the absorption of **DOV**·2OTs. (c) Absorption spectra of a CH₂Cl₂ solution of **TDA** (1.9×10^{-5} M), previously protonated with 3 equivalents of TfOH, upon titration with **DOV**·2OTs. The inset shows the titration curve (black dots) together with the fitting of the data (dashed line).

Chemistry–A European Journal

Research Article
doi.org/10.1002/chem.202203472

Chemistry Europe
European Chemical
Societies Publishing

Electrochemical characterisation: electrochemically induced de-threading

TDA and its association complex with **DOV**·2OTs were characterised in CH₂Cl₂ in the presence of 100-fold excess of TBAOTs by means of cyclic voltammetry and differential pulse voltammetry. In analogy with parent compounds,[5] **TDA** shows irreversible oxidation processes related to the calixarene scaffold at potential values above $+1.4\,V$ versus SCE (Figure S36). In addition, **TDA** also exhibits an irreversible oxidation process related to the dansyl units.[19] **DOV**·2OTs shows two monoelectronic and reversible reduction processes at $-0.42\,V$ and $-0.85\,V$ versus SCE (Figure 6a).

Upon addition of the wheel, the same behaviour previously reported for parent pseudorotaxanes is observed: i) the first process is irreversible, with a cathodic peak shifted to more negative potential values, on account of the host-guest charge transfer interaction; ii) the second process is reversible and at the same potential as the free **DOV**·2OTs; iii) the anodic peak of the first redox process corresponds to the oxidation of the free axle. This behaviour corresponds to a square scheme (Figure 6b), wherein the first reduction of the axle is followed by dissociation of the pseudorotaxane, which then reassembles upon subsequent reoxidation of the free axle. Upon addition of
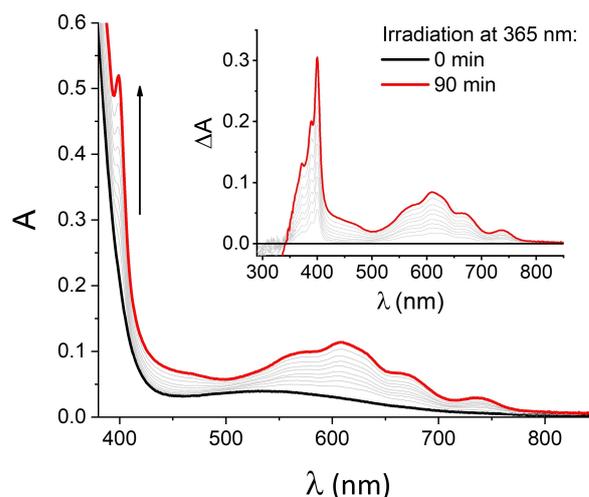
acid, besides a general deterioration of the curves, the same pattern is observed (Figure S40).

Photochemically-induced de-threading

From the photophysical and electrochemical experiments reported above, two features of the system must be highlighted: i) the emission of the dansyl moieties in the pseudorotaxane complex is quenched, most likely by virtue of photoinduced electron transfer from the excited dansyl groups to the bipyridinium unit;[13,19] ii) reduction of bipyridinium results in disassembly of the pseudorotaxane complex. Taken together, these results prompted us to verify the possibility to control the de-threading reaction by means of photoinduced electron transfer. Indeed, upon irradiation of the dansyl moieties, electronic reduction of the bipyridinium should occur, followed by de-threading. Nevertheless, the mechanical motion is in competition with the back electron transfer process from the reduced bipyridinium to the oxidised dansyl. As a matter of fact, upon steady-state irradiation of a solution of the pseudorotaxane, no spectral changes were observed, as the de-threading reaction is much slower than the electronic reset (Figure S43). To accumulate the reduced bipyridinium, a sacrificial mechanism is exploited,[20] by using an external redox reactant that operates after the photoinduced electron transfer. To this aim, a degassed solution of [**TDA**⊃**DOV**]2OTs was irradiated in the presence of an excess of tributylamine as a sacrificial agent. Upon irradiation of the dansyl units at 365 nm, the characteristic absorption features of the bipyridinium radical cation arise over time (Figure 7, see inset), namely two intense and structured bands at 400 nm and 610 nm.

To prove that the reduced bipyridinium de-threads from the calixarene macrocycle, emission spectra were collected, as **TDA** fluorescence is quenched upon complexation. Indeed, the

Figure 6. (a) Diagram with the reduction potentials for the first (black line) and the second process (red line) of **DOV**·2OTs and **TDA**⊃**DOV**·2OTs. The reduction potentials reported are obtained from differential pulse voltammetries.[a] Peak potential of the irreversible process. (b) Schematic representation of the electrochemical square scheme related to the first reduction of the **DOV**·2OTs.

Figure 7. Absorption spectra of an argon-purged CH₂Cl₂ solution of **TDA** (1.3×10^{-4} M), **DOV**·2OTs (2.0×10^{-4} M) and tributylamine (0.05 M) upon irradiation at 365 nm. Inset: Absorption spectra obtained upon subtracting the spectrum before irradiation to the spectra at increasing irradiation times.

Chemistry–A European Journal

Research Article
doi.org/10.1002/chem.202203472

**Chemistry
Europe**
European Chemical
Societies Publishing

emission intensity of the dansyl units of **TDA** increases on irradiation and then decreases on subsequent addition of O_2, as expected upon de-threading and rethreading, respectively (see above). Approximately 10% of the complex is dissociated upon irradiation, as evaluated from the absorption and emission spectra (see Figure 7 and Figure S47). The process is not fully reversible, as a minor photodegradation of **TDA** may occur (see Figure S48). A residual absorption band around 430 nm is observed after one cycle, which is assigned to the degradation products of the oxidised tributylamine (Figure S49).

Conclusion

We have designed, synthesised, and characterised a novel calix[6]arene wheel decorated with dansyl units. The functionalisation with fluorescent sulphonamides moieties has two advantages with respect to former models. First, the fluorescent units can be exploited to monitor the state of the system: both the protonation state and the complexation of the wheel are associated with different fluorescence signals, which can therefore give information on the state of the system, thus facilitating, for instance, the determination of the parameters associated with the threading reaction. Moreover, the dansyl units can be exploited to trigger the de-threading reaction, both chemically and photochemically.

As a matter of fact, the molecular motion (i.e., de-threading) of the pseudorotaxane formed between **TDA** and a bipyridinium-based axle can be triggered by three orthogonal and reversible stimuli, which address either the guest, the host or the complex as a whole: i) electrochemical reduction of the molecular axle (in analogy with parent calixarene-bipyridinium adducts);[5] ii) protonation of the wheel component;[21] iii) photoinduced electron transfer to the encapsulated bipyridinium guest by excitation of the dansyl units of the host.[22] The capability of tuning the supramolecular interactions of molecular machines components by means of multiple independent stimuli opens the possibility to design functionally complex architectures. One of the advantages of multiresponsive systems is their versatility, as they can be operated in principle in different environments; on the other hand, they could also be exploited to implement molecular logic gates,[23] by taking advantage of the multiple inputs (chemical, electrochemical and photochemical) and outputs (electric current, fluorescence, absorbance) associated with their operation.

Experimental Section

Synthesis: Solvents were dried following standard procedures; all other reagents were of reagent grade quality, obtained from commercial sources and used without further purification. Chemical shifts are expressed in ppm using the residual solvent signal as an internal reference. Mass spectra were determined in ESI mode. **TN**, **TTA**, and **DOV·2OTs** were synthesised according to reported procedures.

Absorption and luminescence spectra: UV-vis absorption and luminescence spectra were recorded with a Cary 300 (Agilent) spectrophotometer and a FS5 (Edinburgh) spectrofluorimeter, respectively. Measurements were performed on air-equilibrated CH_2Cl_2 (Sigma-Aldrich) solutions at room temperature, unless otherwise specified. Solutions were examined in 1-cm spectrofluorimetric quartz cells. Luminescence quantum yields were determined using 5-(dimethylamino)naphthalene-1-sulfonamide (dansyl amide) in methanol ($\phi_f = 0.32$) and naphthalene in cyclohexane ($\phi_f = 0.036$) as standards. Luminescence lifetimes were measured with a FLS920 (Edinburgh) time-correlated single-photon counting spectrofluorimeter, exciting the sample at 340 nm with a pulsed laser.

Determination of the stability constants from spectroscopic titrations: Titrations were performed by adding with a microsyringe aliquots of titrant to the solution of titrand. The absorption or emission changes were monitored throughout the titration. The apparent stability constants of the complexes were obtained by fitting the spectra with the software HypSpec,[24] using a 1:1 association model. The titration experiments were repeated at least 2 times and the values of the association constants were averaged.

Kinetic experiments: Reaction's kinetics was investigated by means of a stopped flow spectrometer (Applied Photophysics SX 18-MV). The experimental data were fitted with the software Berkeley-Madonna[25] using a mixed order reaction (second order for threading, first order for de-threading), with the constrain that the ratio between the two rate constants has to be equal to the thermodynamic constant determined from titrations. Multiple experiments were fitted and the values of the kinetic constants were averaged.

Electrochemical measurements: Cyclic voltammetric (CV) and differential pulse voltammetric (DPV) experiments were carried out in argon-purged CH_2Cl_2 (Sigma-Aldrich) with an Autolab 30 multi-purpose instrument interfaced to a PC. The working electrode was a glassy carbon electrode (Amel, 0.07 cm²), carefully polished with an alumina-water slurry on a felt surface, immediately before use. The counter electrode was a Pt wire, separated from the solution by a frit, an Ag wire was employed as a quasi-reference electrode and ferrocene was present as an internal standard. The concentration of the examined compounds was ranging from 0.08 to 0.4 mM. Tetrabutylammonium hexafluorophosphate ($TBAPF_6$) or tetrabutylammonium tosylate (TBAOTs) were added in a 100-fold proportion with respect to the sample concentration, as supporting electrolyte. Cyclic voltammograms were obtained at scan rates varying from 50 to 2000 mV s^{-1}. Differential pulse voltammetries were performed with a scan rate of 20 mV s^{-1} (pulse height 75 mV). The IR compensation was used and every effort was made throughout the experiments in order to minimize the resistance of the solution. The electrochemical reversibility of the voltammetric wave of ferrocene was taken as an indicator of the absence of uncompensated resistance effects.

Photochemical experiments: Irradiation experiments were carried out with a Helios Quartz medium-pressure mercury lamp in argon-purged CH_2Cl_2 solutions. The 365 nm emission line was selected with an interference filter. The incident light intensity was measured using the ferric oxalate actinometer[26] and was of the order of 10^{-8} einstein/s.

Acknowledgements

Chemistry–A European Journal

Research Article
doi.org/10.1002/chem.202203472

Chemistry Europe
European Chemical
Societies Publishing

Conflict of Interest

There are no conflicts to declare.

Data Availability Statement

The data that support the findings of this study are available from the corresponding author upon reasonable request.

[1] a) N. Darwish, A. C. Aragonès, T. Darwish, S. Ciampi, I. Díez-Pérez, *Nano Lett.* **2014**, *14*, 7064–7070; b) S. Attar, D. Espa, F. Artizzu, L. Pilia, A. Serpe, M. Pizzotti, G. Di Carlo, L. Marchiò, P. Deplano, *Inorg. Chem.* **2017**, *56*, 6763–6767; c) B. Doistau, L. Benda, J.-L. Cantin, L.-M. Chamoreau, E. Ruiz, V. Marvaud, B. Hasenknopf, G. Vives, *J. Am. Chem. Soc.* **2017**, *139*, 9213–9220; d) J. Hu, J. S. Ward, A. Chaumont, K. Rissanen, J.-M. Vincent, V. Heitz, H.-P. Jacquot de Rouville, *Angew. Chem. Int. Ed.* **2020**, *59*, 23206.

[2] M. Gaedke, H. Hupatz, H. V. Schröder, S. Suhr, K. F. Hoffmann, Valkonen, B. Sarkar, S. Riedel, K. Rissanen, C. A. Schalley, *Org. Chem. Front.* **2021**, *8*, 3659–3667.

[3] a) M. Baroncini, S. Silvi, A. Credi, *Chem. Rev.* **2020**, *120*, 200–268; b) S. Erbas-Cakmak, D. A. Leigh, C. T. McTernan, A. L. Nussbaumer, *Chem. Rev.* **2015**, *115*, 10081–10206; c) M. Xue, Y. Yang, X. Chi, X. Yan, F. Huang, *Chem. Rev.* **2015**, *115*, 7398–7501.

[4] a) G. Cera, A. Arduini, A. Secchi, A. Credi, S. Silvi, *Chem. Rec.* **2021**, *21*, 1161–1181; b) A. Arduini, G. Orlandini, A. Secchi, A. Credi, S. Silvi, M. Venturi, *Calix-Based Molecular Machines and Devices* in *Reference Module in Chemistry, Molecular Sciences and Chemical Engineering*, **2014**, 1–26.

[5] A. Credi, S. Dumas, S. Silvi, M. Venturi, A. Arduini, A. Pochini, A. Secchi, *J. Org. Chem.* **2004**, *69*, 5881–5887.

[6] G. Cera, M. Bazzoni, A. Arduini, A. Secchi, *Org. Lett.* **2020**, *22*, 3702–3705.

[7] Selected, recent examples of sulfonated calixarenes, see: a) D. Sbravati, A. Bonardi, S. Bua, A. Angeli, M. Ferraroni, A. Nocentini, A, Casnati, P. Gratteri, F. Sansone, C. T. Supuran, *Chem. Eur. J.* **2022**, *28*, e202103527; b) G. Cera, G. Giovanardi, A. Secchi, A. Arduini, *Chem. Eur. J.* **2021**, *27*, 10261–10266; c) Y. S. Park, Y. Kim, K. Paek, *Org. Lett.* **2019**, *21*, 8300–

8303; d) K. D. Daze, M. C. F. Ma, F. Pineux, Fraser Hof, *Org. Lett.* **2012**, *14*, 1512–1515; e) T. Pinter, S. Jana, R. J. M. Courtemanche, F. Hof, *J. Org. Chem.* **2011**, *76*, 3733–3741.

[8] Selected examples of dansylated calixarenes, see: a) B. Uttam, S. Polepalli, S. Sinha, A. Majumder, C. Pulla Rao, *ACS Appl. Nano Mater.* **2022**, *5*, 11371–11380; b) N. Qureshi, D. S. Yufit, K. M. Steed, J. A. K. Howard, J. W. Steed, *CrystEngComm* **2014**, *16*, 8413–8420; c) S. Pandey, A. Azam, S. Pandey, H. M. Chawla, *Org. Biomol. Chem.* **2009**, *7*, 269–279; d) A. Dhir, V. Bhallaand, M. Kumar, *Org. Lett.* **2008**, *10*, 4891–4894; e) N. M. Buie, V. S. Talanov, R. J. Butcherand, G. G. Talanova, *Inorg. Chem.* **2008**, *47*, 3549–3558.

[9] For dansyl-based macrocyclic sensors, see for example: R. Kumar, A. Sharma, H. Singh, P. Suating, H. S. Kim, K. Sunwoo, I. Shim, B. C. Gibb, J. S. Kim, *Chem. Rev.* **2019**, *119*, 9657–9721 and references therein.

[10] Y.-H. Li, L.-M. Chan, L. Tyer, R. T. Moody, C. M. Himel, D. M. Hercules, *J. Am. Chem. Soc.* **1975**, *97*, 3118–3126.

[11] See: B. Valeur, M. N. Berberan-Santos, M. M. Martin, P. Plaza, in *Analytical Methods in Supramolecular Chemistry*, 2nd ed.,(Ed.: C. A. Schalley), John Wiley & Sons **2012**, pp. 287–336.

[12] F. Vögtle, S. Gestermann, C. Kauffmann, P. Ceroni, V. Vicinelli, L. De Cola, V. Balzani *J. Am. Chem. Soc.* **1999**, *121*, 12161–12166.

[13] I. Pisagatti, D. Crisafulli, A. Pappalardo, G. Trusso Sfrazzetto, A. Notti, F. Nastasi, M. F. Parisi, N. Micali, G. Gattuso, V. Villari, *Mater. Today Chem.* **2022**, *24*, 100841.

[14] J. De Mendoza, M. Carromolino, F. Cuevas, P. M. Nieto, P. Prados, D. N. Reinhoudt, W. Verboom, R. Ungaro, A. Casnati, *Synthesis* **1994**, *1994*, 47–50.

[15] S. Kanamathareddy, C. D. Gutsche, *J. Org. Chem.* **1994**, *59*, 3871–3879.

[16] A precise quantification of the ratio of the pseudorotaxane species present in the solution was prevented by the signals broadness.

[17] M. Montalti, L. Prodi, N. Zaccheroni, G. Falini, *J. Am. Chem. Soc.* **2002**, *124*, 45, 13540–13546.

[18] A. Arduini, R. Bussolati, A. Credi, A. Pochini, A. Secchi, S. Silvi, M. Venturi, *Tetrahedron* **2008**, *64*, 8279–8286.

[19] P. Ceroni, I. Laghi, M. Maestri, V. Balzani, S. Gestermann, M. Gorka, F. Vögtle, *New J. Chem.* **2002**, *26*, 66–75.

[20] P. R. Ashton, R. Ballardini, V. Balzani, A. Credi, K. R. Dress, E. Ishow, C. J. Kleverlaan, O. Kocian, J. A. Preece, N. Spencer, J. F. Stoddart, M. Venturi, S. Wenger, *Chem. Eur. J.* **2000**, *6*, 3558–3574.

[21] a) S. Cherraben, J. Scelle, B. Hasenknopf, G. Vives, M. Sollogoub, *Org. Lett.* **2021**, *23*, 7938–7942; b) A. E. Kaifer, W. Li, S. Silvi, V. Sindelar, *Chem. Commun.* **2012**, *48*, 6693–6695.

[22] A. Credi, B. Ferrer, *Pure Appl. Chem.* **2005**, *77*, 1051.

[23] See e.g.: a) D. C. Magri, *Coord. Chem. Rev.* **2021**, *426*, 213598–213611; b) S. Erbas-Cakmak, S. Kolemen, A. C. Sedgwick, T. Gunnlaugsson, T. D. James, J. Yoon, E. U. Akkaya, *Chem. Soc. Rev.* **2018**, *47*, 2228 and references therein.

[24] http://www.hyperquad.co.uk/.

[25] https://berkeley-madonna.myshopify.com/.

[26] C. G. Hatchard, C. A. Parker, *Proc. R. Soc. London* **1956**, *A235*, 518–536.